1996 Conf. on Oceanic and Atmospheric Predictions Atlanta, Amer. Meteor. Soc., 281-286

An Operational Forecast Model for Extratropical Storm Surges along the U.S. East Coast

Sung-Chan Kim[1], Jye Chen, and Wilson A. Shaffer
Techniques Development Laboratory
Office of System Development
National Weather Service, NOAA
Silver Spring, Maryland

ABSTRACT

To complement the existing statistical extratropical storm surge guidance for the U.S. East Coast, the Techniques Development Laboratory (TDL) has developed a dynamic forecast model. The model is based on the depth-integrated shallow water equations as in the National Weather Service's (NWS) Sea, Lake, and Overland Surges from Hurricanes (SLOSH) model. The calculation domain covers three main oceanographic regions--the Gulf of Maine, the Mid Atlantic Bight, and the South Atlantic Bight--and includes Long Island Sound, Delaware Bay, and Chesapeake Bay. The surge model is forced by surface winds and pressures generated by NWS's Aviation (AVN) model. The model starts from a water level initialized at 0 ft and undergoes 48-hour spinup period. During this period, past 12-hourly analyzed AVN fields drive the surge model. Once the spinup period is complete, surge computations are performed based on AVN forecasts of winds and pressures.

In a hindcast of the Halloween Storm of 1991, computed surge heights from the model compare favorably with tide gage observations. The surge model was run in an NWS forecast operational mode during the 2-day extratropical event of March 1994. With the updated AVN model forecasts every 12 hours, 36-hour surge forecasts were produced. The results show that operational storm surge forecasting is promising with this model.

1. Introduction

The U.S. East Coast is vulnerable to the damage caused by extratropical storms, commonly known as Northeasters or Nor'easters, which prevail between fall and spring (e.g., Dolan and Davis 1992). Along the East Coast, extratropical storm surges over 1 m occur almost once a year and surges over 0.5 m are seen several times a year. The surges, combined with high waves, are disastrous to coastal communities, causing flooding, beach erosion, and destruction of engineered structures.

The National Weather Service (NWS) warns coastal residents of threatening conditions due to extratropical storms. The forecasting of coastal surge heights from extratropical storms is prerequisite to the preparation for the impact. The NWS has maintained a statistical forecast model for approximately 20 years. Statistical relationships were derived relating surge heights for 13 coastal locations to offshore pressure gradients. These relationships were then applied to NWS model forecasts of pressure, yielding storm surge forecasts (Pore et al. 1974). Although the statistical model serves as a good guidance tool, it lacks continuous information both in time and in space. A dynamic model will fill this gap and provide better understanding of the physics of the process.

For tropical storms, the NWS developed a dynamic surge forecast model SLOSH--Sea, Land, and Overland Surges from Hurricanes (Jelesnianski et al. 1992). There are major differences between tropical and extratropical surges that separate modeling approaches for the two. The time and length scales involved with extratropical storms are larger than the scales for tropical storms. The tropical storm surge dynamics thus are transient in nature while the extratropical surges are further complicated by the additional quasi-stationary characteristics. The cross-shore transports dominate for the tropical storm surges while the longshore transport becomes more important for the extratropical storm surges, meaning much influence from ambient wind field well away from the "center" of the system. Thus, extratropical storm surge models, unlike the models for the tropical storm surges, cannot rely on simplified parametric wind fields.

A storm surge is primarily a barotropic response of coastal water to the atmospheric forces (e.g., Murty 1984) and the surge dynamics is controlled by varying bottom topography and coastline geometry (e.g., Platzman 1963). Thus, having reasonable atmospheric forcing and basin topography becomes critical to the success of a surge model. For the atmospheric forcing, we have taken advantage of the NWS's existing Aviation (AVN) model (Kalnay et al. 1990). The NWS's extensive set of coastal topography databases, from the SLOSH model basins along the U.S. East Coast (Fig. 1) aided us in developing a model basin

[1] Research and Data Systems, Inc., Greenbelt, Maryland.

for the U.S. East Coast extratropical storm surge model. In this study, we pose an *a priori* assumption that the secondary factors to the surge dynamics, including the non-linear advection and surge-tide interaction, have minimal impact on the open coast but may be important for enclosed or semi-enclosed water bodies.

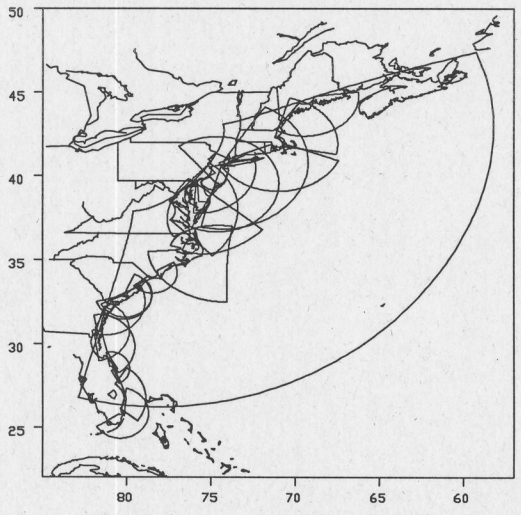

Figure 1. Location of the East Coast surge model basin (the largest domain) with 20 operational SLOSH basins (smaller domains) along the U.S. East Coast.

The objective of this study is to investigate the feasibility of an operational dynamic forecast model for extratropical storm surges. A secondary objective is to study the characteristics of the extratropical storm surges along the U.S. East Coast. We intend to determine the response conditions to meteorological forcing and coastal geomorpho-hydrodynamics. A dynamic model is built upon the depth-integrated quasi-linear shallow water equations for a one-layer barotropic ocean, subject to surface forcing and bottom friction. An analytic grid is generated, featuring a high resolution coastline. We first ran the model for the hindcast of coastal surges from the Halloween Storm of 1991 to investigate whether coastal water levels respond properly to the atmospheric forcing of the AVN analysis fields. The model then was run as it would be in NWS operations for the 2-day period of the 1994 March extratropical event.

2. Governing Equations

Following Platzman (1963), the shallow water equations are written in cartesian coordinates:

$$\frac{\partial M}{\partial t} = -g(D+h)\left[B_r \frac{\partial (h-h_0)}{\partial x} - B_i \frac{\partial (h-h_0)}{\partial y} \right] + f(A_r N + A_i M) + C_r \tau_x - C_i \tau_y \quad (1)$$

$$\frac{\partial N}{\partial t} = -g(D+h)\left[B_r \frac{\partial (h-h_0)}{\partial y} + B_i \frac{\partial (h-h_0)}{\partial x} \right] - f(A_r M - A_i N) + C_r \tau_y + C_i \tau_x \quad (2)$$

$$\frac{\partial h}{\partial t} = -\frac{\partial M}{\partial x} - \frac{\partial N}{\partial y} \quad (3)$$

Nonlinear advective terms and horizontal viscosity terms are neglected in the above equations. The equations are to be closed for (M,N), the volume transport in the (x,y)-directions, and h, the water surface elevation above the reference datum. Here, we define variables such as (τ_x,τ_y), the surface stresses in (x,y)-directions; h_0, hydrostatic elevation; D, water depth below datum; f, the Coriolis parameter; and g, the gravitational acceleration. By using a slip condition at the bottom boundary and constant eddy viscosity (Jelesnianski 1967), the complex friction parameters, A, B, and C are related to the bottom stresses through the Ekman number ($\varepsilon = D\,(f/2\nu)^{1/2}$). Here, ν is the kinematic eddy viscosity and the subscripts r and i denote real and imaginary parts, respectively.

Following Jelesnianski et al. (1992), a grid transformation is generated which maintains high resolution spacing near the coast while achieving computational economy. Through a simple analytic grid transformation, orthogonality of the grid basis functions is retained so that the governing equations have only a few additional terms. Consider the conformal transformation from $z = (x,y)$ to $\zeta = (P,Q)$:

$$z = R\cdot(e^{\zeta} + \gamma\cdot e^{-\zeta}) \quad (4)$$

Here, $R > 0$. The coordinate system is polar for $\gamma = 0$, elliptical for $0 < |\gamma| < 1$, and hyperbolic for $\gamma = \pm 1$. Then, the transport (M,N) is transformed to (U,V) by

$$(U,V) = \left(\frac{dz}{d\zeta}\right)^{*} (M,N) \quad (5)$$

Here, the asterisk denotes the complex conjugate.

The transport equations are transformed to the new (P,Q) coordinate system:

$$\frac{\partial U}{\partial t} = -g(D+h)(B_r\frac{\partial h}{\partial P} - B_i\frac{\partial h}{\partial Q}) + f(A_r V + A_i U) + \left[Re(\frac{dz}{d\zeta})^*\right]T_x - \left[Im(\frac{dz}{d\zeta})^*\right]T_y \quad (6)$$

$$\frac{\partial V}{\partial t} = -g(D+h)(B_r\frac{\partial h}{\partial Q} + B_i\frac{\partial h}{\partial P}) - f(A_r U - A_i V) + \left[Re(\frac{dz}{d\zeta})^*\right]T_y + \left[Im(\frac{dz}{d\zeta})^*\right]T_x \quad (7)$$

$$\frac{\partial h}{\partial t} = -\left|\frac{d\zeta}{dz}\right|^2 \cdot (\frac{\partial U}{\partial P} + \frac{\partial V}{\partial Q}) \quad (8)$$

where the atmospheric forcing terms are

$$T_x = g(D+h)(B_r\frac{\partial h_0}{\partial x} - B_i\frac{\partial h_0}{\partial y}) + C_r\tau_x - C_i\tau_y \quad (9)$$

$$T_y = g(D+h)(B_r\frac{\partial h_0}{\partial y} + B_i\frac{\partial h_0}{\partial x}) + C_r\tau_y + C_i\tau_x \quad (10)$$

Note that T_x and T_y are defined on the (x,y) coordinate, not on the (P,Q) coordinate.

3. Model basin grid and topography

The East Coast is composed of three distinct characteristic oceanographic regions--the Gulf of Maine (GOM), the Mid Atlantic Bight (MAB), and the South Atlantic Bight (SAB). The MAB contains three major embayments--Long Island Sound, Delaware Bay, and Chesapeake Bay. The MAB has experienced the most extratropical storm surge events, followed by the GOM. The barotropic response of the MAB and the GOM to local alongshore winds is known to be the major cause for the winter variability of the coastal water elevation (e.g., Wang 1979; Vermesch et al. 1979). Beardsley and Haidvogel (1981) showed that the water level from a linear model of integrated shallow water equations with adiabatic boundary conditions responds realistically in the MAB but is more subject to boundary conditions in the GOM. Wright et al. (1986) also showed the dependency of the barotropic response in the GOM on the boundary condition on the Scotian Shelf. The extratropical events are far less pronounced in the SAB, which compared to those in the MAB (e.g., Menzel 1993).

In our surge model, we concentrate primarily on the MAB with its embayments and secondarily on the GOM. For the few extratropical events which impost the southern Atlantic states, the SAB is included, with the southern boundary extending to the Florida Keys. To avoid boundary condition problems associated with the GOM we extend the northern boundary past Nova Scotia. A hyperbolic grid with dimensions of 120 by 85 was generated (Fig. 1). The grid spans approximately 25°N to 50°N and 57°W to 82°W. The grid size varies from approximately 3 km near the MAB coast to approximately 10 km along the shelf edge.

Depth data from the National Geophysical Data Center (NGDC) with 5 minute resolution were combined with the existing SLOSH basin database and interpolated onto the computational grid. In contrast to enclosed domains such as the Great Lakes or semi-enclosed regions such as the North Sea, the U.S. East Coast has wide open coasts. This causes the model to be sensitive to boundary conditions. Because of the increased baroclinic effect off the shelf, we limit the calculations to the continental shelf, thus confining the dynamics to the barotropic problem. General consensus is that the open boundary lies along the continental shelf edge (e.g., Heaps 1983). The open boundary is set at the 500 m depth contour. Figure 2 shows the model computational area. AVN grid points used for the computation are marked by crosses. The selected monitor points for tide gage stations are marked by a to f: a) Boston, Massachusetts; b) Montauk, New York; c) Port Jefferson, New York; d) Willets Point, New York; e) Sandy Hook, New York; and f) Atlantic City, New Jersey.

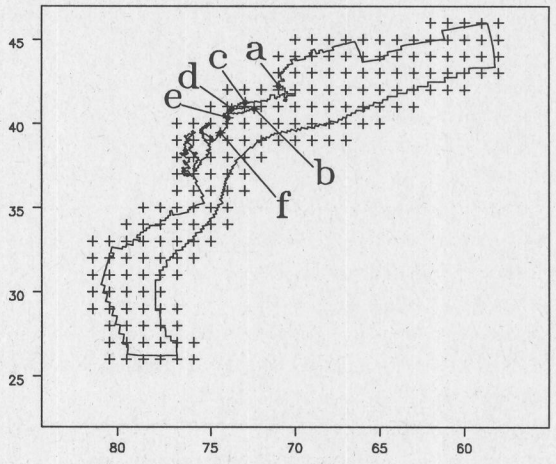

Figure 2. Extratropical model computational area.

4. Atmospheric forcing

We use the National Weather Service's Aviation (AVN) model of 126 spectral components, interpolated onto

1-degree latitude by 1-degree longitude grid boxes. The mean sea level pressures and the lowest sigma-level winds are used. The mean sea level pressure given by the AVN model is obtained after removing the orographic effects induced by the model's terrain. The model topography shows the steep drop-off seaward of the coasts of MAB and lower GOM. One may argue that the coastline from the 1-degree AVN model terrain differs from the actual coastline, thus the model winds near the coasts do not reflect accurate values. But, we are optimistic about the AVN wind fields which are computed with dynamic consistency within the model. The lowest sigma level wind is representative of the wind at approximately 30-m elevation.

The AVN forecasts begin for analyses at 0000 UTC and 1200 UTC each day and are available on NOAA's computers. Six hourly forecasts are available on the NAS-9000 computer, whereas 3 hourly forecasts are available on C90-Cray platform. At the present time, we operate on the NAS-9000 where 6-hourly forecasts are used. The AVN output is in the WMO's (World Meteorological Organization) GRIB format (Stackpole 1994). Surface pressure and wind are extracted for a 35° × 35° window. Figure 2 shows the actual 1° × 1° points used to drive the surge model. Analysis fields are saved for use in the hindcast of the next time projection.

5. Numerical schemes

We utilize Mesinger and Arakawa's (1976) 'B' grid scheme to solve the governing equations: surge height is calculated at the center of a grid cell and transports are calculated at corner points of a cell. The 'B' scheme has an advantage in dealing with Coriolis and advective terms. Along the open boundary, water level is set to the inverted barometric pressure. Test results with a radiation boundary condition at the open boundary showed little effect on the coastal surges as compared to those from the hydrostatic boundary condition. We impose a zero transport condition at land boundaries. Since the 'B' scheme causes noise, especially near the zig-zag boundaries, the model requires the application of spatial smoothing. Pressure from the AVN model is interpolated onto the height points while the winds and pressure gradients are interpolated to the momentum points.

The forward-backward time difference scheme of Mesinger and Arakawa (1976) is used: Water level is updated first from the continuity equation, then transports are calculated. The C-F-L stability conditions show that a time step of 120 seconds is sufficient. For the spinup from a quiescent sea of mean sea level to fully applied surface wind stresses, a cosine tapering function is used. We set 8 hours as the minimum spinup time. The wind stresses and pressures are interpolated linearly in time between the AVN models's 12-hour analysis or 6-hour forecast fields. All the friction coefficients are the same as in the SLOSH model (Jelesnianski et al. 1992). Astronomical tide is not computed in this model. Superposition of astronomical tide levels and storm surge values is assumed, giving the total water levels.

6. Hindcast of Halloween Storm of 1991

The Halloween Storm of 1991 occurred between October 28 and November 1, 1991. Storm surge, accompanied by storm-generated waves, raked the U.S. East Coast and caused extensive damage from Maine to North Carolina. This storm had unusual characteristics; a low pressure center deepened in the open ocean and moved westward toward the coast, then southward along the coast, and finally developed into a tropical system (Fig. 3). Most extratropical systems along the U.S. East Coast move seaward from the coastline. We chose this storm for the hindcast because of its well assessed impact to the coastal region and the availability of AVN model forecasts from NWS and tide gage data from the Office of Ocean and Earth Sciences, National Ocean Service (NOS).

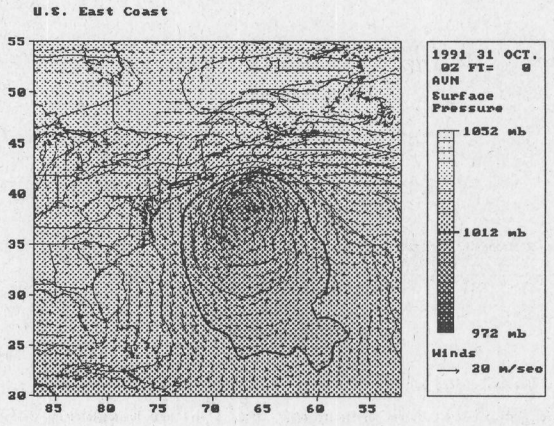

Figure 3. Surface Pressure and winds at 0000 UTC, October 31, 1991 during the Halloween Storm.

The hindcast period spans 5 days from 0000 UTC 28 October 1991 to 0000 UTC 2 November 1991. We selected six tide gage stations for displaying results. Boston, Massachusetts represents the surge behavior in the GOM. Port Jefferson, New York and Willets Point, New York are located in the Long Island Sound. Three gage stations--Montauk, New York, Sandy Hook, New York, and Atlantic City, New Jersey--were picked to investigate the temporal and spatial relationships along the upper MAB. The observed storm surge is defined as the observed tide height minus the astronomical tide level. The gage-measured surges for the 120-h period are compared to hindcast values of surge height for the monitor points (Fig. 4). The

near tidal-frequency motion monitored at Boston can be related to the natural frequency of Gulf of Maine basin. We attribute the underestimated peak surge height at Boston to either an underforecast of coastal wind speeds in the Gulf of Maine or to the tide gage location inside Boston Harbor. The model surge heights, in general, are in phase and in good agreement with the ones from tide gage readings, especially for the locations along the open coast. The arrival time of the peak surge at each gage location is closely related to the storms's position and intensity. The model captures the relatively quick decrease in surge heights as the storm weakened and moved away from the coast.

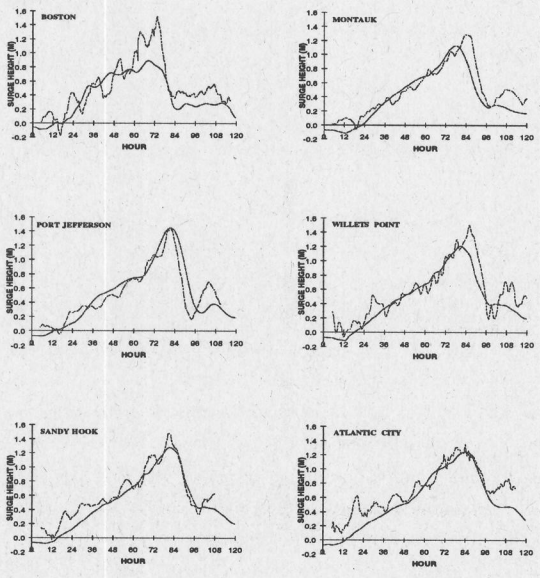

Figure 4. Hindcast surge heights at six monitoring points. Solid and dashed lines represent the observation and model output, respectively.

7. Forecast simulation during March 1994 extratropical event

Between 0000 UTC 1 March 1994 and 0000 UTC 4 March 1994, there was a typical extratropical event in which a low pressure system moved northeastward while intensifying (Fig. 5). During this period, we kept in close contact with the NWS office at Atlantic City, New Jersey. Every 12-h cycle, we ran the model for 48 hour 'hindcast' with analyses fields in 12 hour intervals and 36 hour 'forecast' in 6 hour intervals (Fig. 6). The forecasts were sent in real time to the Atlantic City office and were later compared with the tide gage observations (Fig. 7). These forecasts were provided to the NWS's forecast office in Atlantic City as guidance for their forecast preparation.

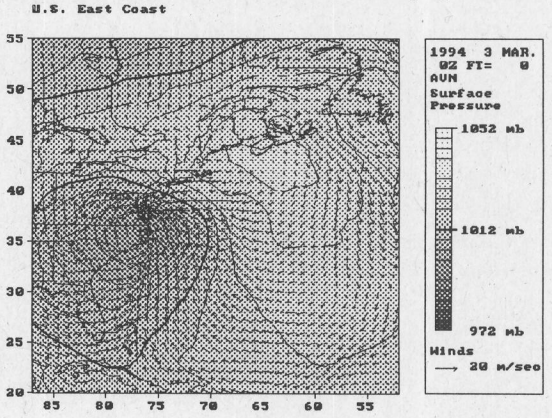

Figure 5. Surface pressure and winds at 0000 UTC, March 3, 1994, during March '94 event.

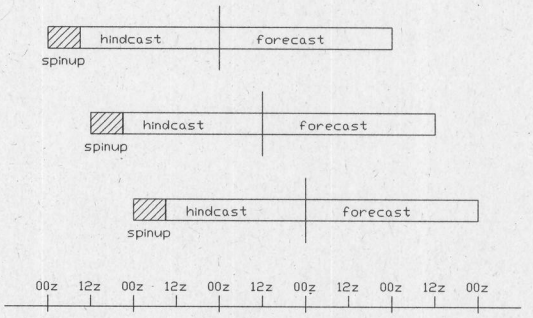

Figure 6. NWS operational schedule for the East Coast surge model. The 48-h hindcast is initialized from quiescent water using 8-h spinup. The maximum forecast projection of 36 hours was later extended to 48 hours.

The forecasts fare well with the observations. The first values in each forecast show results from hindcasts, bringing water levels to their "initial" values. We notice that the hindcast for 1200 UTC of 3/3/94 is off by almost .3 m from the observation. This is mainly due to the linear time interpolation between the 12-h analyses in the 'hindcast' mode. For slow moving storms, this effect would be negligible. Fast moving storm events, however, would require better time interpolation schemes. One temporary remedy is to use the 6-h forecast fields inserted between analyses fields. This, however, is based on the assumption that the 6-h forecast adequately describes the state of the atmosphere. We have been developing a composite-interpolation scheme in which a translation vector is defined for the center of a cyclone. For operational use, however, we feel the linear time interpolation is adequate for forecasting purposes because the forecast fields are available with shorter time intervals than hindcast fields.

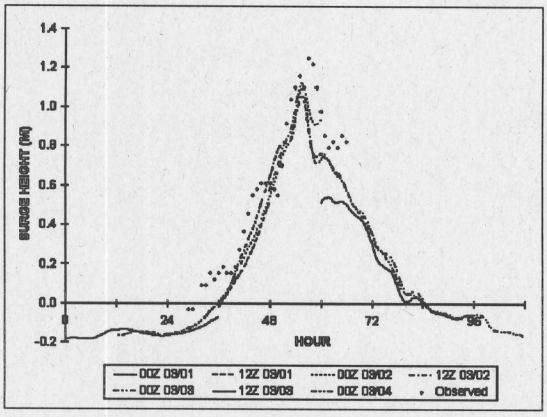

Figure 7. Forecast of storm surges for Atlantic City, New Jersey, during March '94 extratropical event.

8. Conclusions

The quasi-linear depth-integrated barotropic model gives a good, first-order approximation of the coastal surge heights from extratropical storms. The numerical grid used in this study provides detailed information of the water level variation along the coastline. The most critical input--the wind field--provided by the AVN model appears to be adequate for the operational surge hindcast/forecast modeling. The hindcast of the 1991 Halloween Storm shows good agreement with tide gage observations both in amplitude and phase. The simulated operation during the March 1994 extratropical event demonstrates that the model is feasible for use in forecasting.

Acknowledgements

This work has been funded by NOAA's Coastal Ocean Program. We thank NOAA's Ocean Products Center for providing AVN model verification statistics and constructive advice.

REFERENCES

Beardsley, R. C., and D. B. Haidvogel, 1981: Model studies of the wind-driven transport circulation in the Middle Atlantic Bight. *J. Phys. Oceanogr.*, 11, 355 - 375.

Dolan, R., and R. E. Davis, 1992: Rating Northeasters. *Mariners Weather Log*, Winter 1992, National Oceanic and Atmospheric Administration, U.S. Department of Commerce, 4-11.

Heaps, N. S., 1983: Storm surges, 1967 - 1982. *Geophys. J. Roy. Astr. Soc.*, 74, 331 - 376

Jelesnianski, C. P., 1967: Numerical computation of storm surges with bottom stress. *Mon. Weather Rev.*, 95, 740-756.

Jelesnianski, C. P., J. Chen, and W. A. Shaffer, 1992: SLOSH: Sea, lake, and overland surges from hurricanes. *NOAA Tech. Rep. NWS 48*, National Oceanic and Atmospheric Administration, U.S. Department of Commerce, 71 pp.

Kalnay, E., M. Kanamitsu, and W. E. Baker, 1990: Global numerical weather prediction at the National Meteorological Center. *Bull. Amer. Meteor. Soc.*, 71, 1410-1428.

Menzel, D. W., 1993: Ocean processes: U.S. Southeast continental shelf. *DOE/OSTI-11674*, Skidaway Inst. Oceanogr., 112 pp.

Mesinger, F., and A. Arakawa, 1976: Numerical methods used in atmospheric models. Global Atmospheric Research Programme, WMO-ICSU Joint Organizing Committee, *GARP Pub. Ser. No. 17*, World Meteorological Organization, 64 pp.

Murty, T. S., 1984: Storm surge. *Bull. 212, Dept. Fish. Oceans*, Canada, 597 pp.

Platzman, G. W., 1963: The dynamical prediction of wind tides on Lake Erie. *Meteorological Monographs*, 4 (26), American Meteorological Society, 44 pp.

Pore, N. A., W. S. Richardson, and H. P. Perrotti, 1974: Forecasting extratropical surges for the northeast coast of the United States. *NOAA Technical Memorandum NWS TDL-50*, National Oceanic and Atmospheric Administration, U.S. Department of Commerce, 70 pp.

Stackpole, J. D., 1994: A guide to GRIB. *FM-92, National Meteorological Center*, National Weather Service, NOAA, U.S. Department of Commerce, 37 pp.

Vermesch, J. A., R. C. Beardsley, and W. S. Brown, 1979: Winter circulation in the western Gulf of Maine. Part 2: Current and pressure observations. *J. Phys. Oceanogr.*, 9, 768 - 784.

Wang, D. -P., 1979: Low frequency sea level variability on the Middle Atlantic Bight. *J. Mar. Res.*, 37, 683 - 697.

Wright, D. G., D. A. Greenberg, J. W. Loder, and P. C. Smith, 1986: The steady-state barotropic response of the Gulf of Maine and adjacent regions to surface wind stress. *J. Phys. Oceanogr.*, 16, 947 - 966.